Solvent Effect on the Glass Transition Temperature of Syndiotactic Polystyrene Viewed from Time-Resolved Measurements of Infrared Spectra at the Various Temperatures and Its Simulation by Molecular Dynamics Calculation

Akiko Yoshioka and Kohji Tashiro*

Department of Macromolecular Science, Graduate School of Science, Osaka University, Toyonaka, Osaka 560-0043, Japan

Received October 7, 2003; Revised Manuscript Received November 4, 2003

ABSTRACT: Time-resolved infrared spectral measurement was performed in the solvent-induced crystallization process of syndiotactic polystyrene (sPS) glass at the various temperatures, and the crystallization kinetics were analyzed quantitatively. Both of the crystallization rate constant and the crystallinity estimated after passage of long time were found to decrease with decrease in the crystallization temperature. The extrapolation of the rate constant and the crystallinity to the zero values allowed us to estimate the glass transition temperature (T_g) in the organic solvent atmosphere. The T_g of the original glass sample (ca. 100 °C) was found to shift to -90 ± 10 °C for chloroform, -70 ± 10 °C for benzene, and -30 ± 10 °C for toluene. The solvent with higher solubility or higher interaction with sPS was found to shift the T_g at higher degree. To understand this plasticizing effect of solvent from the microscopic point of view, the molecular dynamics calculation was performed for sPS−toluene and sPS−chloroform systems, and a good correspondence was obtained about the T_g shift between the observed and calculated results.

Introduction

The glass transition temperature (T_g) of syndiotactic polystyrene (sPS) is about 100 °C.[1−9] But the sPS glass is known to crystallize even at room temperature when the sample is exposed into an atmosphere of solvent such as chloroform, benzene, toluene, etc.[10−41] The thus-created crystal form is called the δ form, in which the sPS chains of regular $(TTGG)_2$ helical conformation are packed together with solvent molecules to form a so-called complex.[10−39] In the previous papers,[28,30,31,34,38,39] we traced the structural evolution process in this solvent-induced crystallization phenomenon through the time-resolved measurements of infrared and Raman spectra and X-ray scattering. Even when the crystallization experiment was performed at room temperature, the amorphous chains were found to activate their micro-Brownian motion immediately after the migration of solvent molecules into the amorphous region, inducing the regularization of random coils into the T_2G_2 helical conformation. In other words, the crystallization is induced as a result of remarkably large shift of T_g from 100 °C to room temperature or even much lower temperature due to the plasticizing effect of solvent. But it was not possible at that time to estimate the amount of T_g shift in a concrete manner. We investigated the crystallization process in a toluene atmosphere by carrying out the time-resolved infrared spectral measurement at various temperatures.[42] By quantitatively analyzing the time dependence of the crystallization-sensitive band intensity on the basis of Avrami's equation

$$X = 1 - \exp(-k^n t^n) \qquad (1)$$

where X is the degree of crystallinity and t is a time; the apparent crystallization rate constant k and Avrami's index n were evaluated as functions of temperature. (Since the crystallization occurs in a complicated manner including the diffusion of solvent molecules in the amorphous region and so on, it is not certain whether the solvent-induced crystallization phenomenon can be treated by assuming the Avrami-type equation. Therefore, the rate constant k obtained from eq 1 is only *apparent*.[42]) The k value was found to decrease almost linearly with decreasing temperature. Under the assumption that the crystallization is ceased practically when the glassy sample is cooled to T_g, the plot of the k value, more strictly speaking the logarithm of k vs temperature, was extrapolated to the quite small value of 10^{-5} s^{-1}, by which the T_g was estimated to be ca. −20 °C for the sPS−toluene system. (The extrapolation to $k = 10^{-6}$ s^{-1} seems better for the estimation of T_g, as will be discussed in the present paper.)

In this way, on the basis of the crystallization kinetics data collected at the various temperatures, we estimated the toluene-induced T_g shift of sPS glass sample. It is known that the different kind of solvent gives the largely different crystallization rate when the crystallization phenomenon is observed at the same temperature.[31] How different is the T_g shift for the different kind of solvent? In the present paper we will compare the crystallization behavior of sPS glass for chloroform, benzene, and toluene through the time-resolved infrared spectral measurement and estimate the shift of T_g for these individual cases. Of course, the T_g shift may be estimated more directly by performing the viscoelastic measurement in the solvent atmosphere, for example. But it is a little awful to carry out this type of measurement because a toxic organic solvent is used in a large volume in order to expose the sample in the solvent vapor atmosphere.[34] It is more convenient to use

* Corresponding author. E-mail: ktashiro@chem.sci.osaka-u.ac.jp.

10.1021/ma035505z CCC: $27.50
Published on Web 12/18/2003

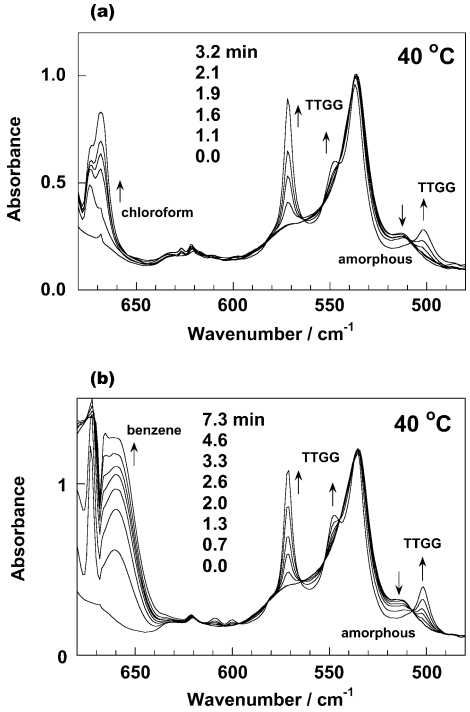

Figure 1. Time dependence of infrared spectra measured in the solvent vapor atmosphere at 40 °C for (a) sPS−chloroform and (b) sPS−benzene systems.

the technique of in-situ infrared spectral measurement for the evaluation of solvent-induced T_g shift, as will be described in the present paper.

The shift of T_g is considered to originate from the strong interaction of sPS chains with solvent molecules. By carrying out the molecular dynamics (MD) calculation for the sPS amorphous model with and without organic solvent molecules taken into account, the T_g shift may be estimated from the microscopic point of view. In the second part of this paper, the MD calculation result is described and is compared with the experimental data in order to understand the plasticizing effect of solvent in a concrete manner.

Experimental Section

Samples. sPS samples (M_w 203 000, M_w/M_n 3.01) were supplied by Idemitsu Petrochemical Co. Ltd., Japan. Glassy samples were prepared by quenching the melt (280−300 °C) into an ice water bath. The amorphous content was checked by infrared spectra.

Time-Resolved Infrared Measurement. The time-resolved infrared spectral measurement was performed in the solvent-induced crystallization process. The optical cell with a solvent reservoir was used for the measurement, the details of which were reported in the previous papers.[31,42] A heater was attached to the cell walls for the measurements at high temperatures. The cell was cooled by ice−water bath when the measurement was made below room temperature. The temperature was monitored by a thermocouple contacted directly to the sample. The infrared spectra were measured at a resolution power 2 cm^{-1} by using a Digilab (Bio-Rad) FTS-60A FT-IR spectrometer equipped with an MCT (mercury−cadmium−telluride) semiconductor detector.

Results and Discussion

Experimental Evaluation of T_g Shift. Figure 1a shows the time dependence of infrared spectra measured at 40 °C in the crystallization process of sPS glass sample in the chloroform vapor atmosphere. As already described in the previous paper,[31] the bands of chloroform appeared at first, and the crystallization-sensitive bands of sPS started to appear with some time delay, indicating an existence of induction time for the crystallization. This can be seen more clearly in Figure 2, where the integrated intensity of the crystalline band at 572 cm^{-1} is plotted against time. (The intensity was reduced by dividing it by the intensity of an internal standard band at 1150 cm^{-1} which did not show any crystallinity dependence.) As the temperature was lowered, the induction time was longer and the growing rate of band intensity was decreased. After a passage of long time the infrared band intensity was almost saturated. The saturated intensity was lower at lower crystallization temperature. In principle, the saturated intensity might be almost equal independent of the crystallization temperature as long as the crystallization is observed for an infinitely long time even when the crystallization proceeds quite slowly at a low crystallization temperature. But this is not practical. We will have to wait for hours to days before getting the saturated band intensity at such a low temperature. In Figure 2 it is not bad to assume actually that the band intensity is almost saturated in a time range of 1 h. Then the band intensity at 40 min after the start of crystallization was plotted against the crystallization temperature as shown in Figure 3, where the band intensity was reduced by the intensity of the 1150 cm^{-1} internal standard band. Although the reduced band intensity is far from zero as seen in Figure 3, the linear extrapolation was made as a trial to estimate the temperature at which the crystallization did not occur any more, giving the T_g of -90 ± 10 °C. (In this linear extrapolation the linear correlation coefficient was 0.9.)

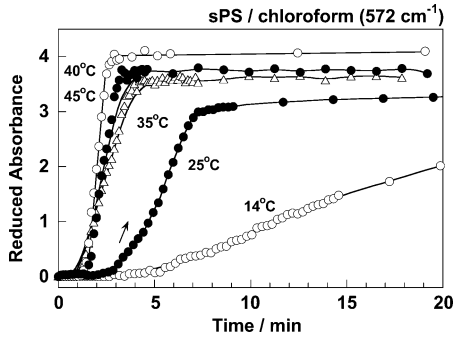

Figure 2. Time dependence of the 572 cm^{-1} band intensity estimated at the various temperatures for the sPS−chloroform system, where the intensity was reduced by the intensity of the 1150 cm^{-1} standard band.

In the previous paper[42] we analyzed the time evolution curve of crystallinity on the basis of Avrami's equation and obtained the k value as a function of crystallization temperature, although the thus-estimated k value is only an apparent one because the crystallization process includes many such complicated factors as diffusion of solvent molecules to take into consideration. A similar treatment was made for the present experimental data. As mentioned in that paper, the infrared intensity as a function of time was normalized and the plot of $\log[-\ln(1 - X)]$ vs $\log(t)$ was made on the basis of the equation

$$\log[-\ln(1 - X)] = n \log(k) + n \log(t) \qquad (2)$$

From this plot the rate constant k was estimated as shown in Figure 4a. An extrapolation to the temperature region of negligibly small k value (ca. 10^{-6} s^{-1}) gives

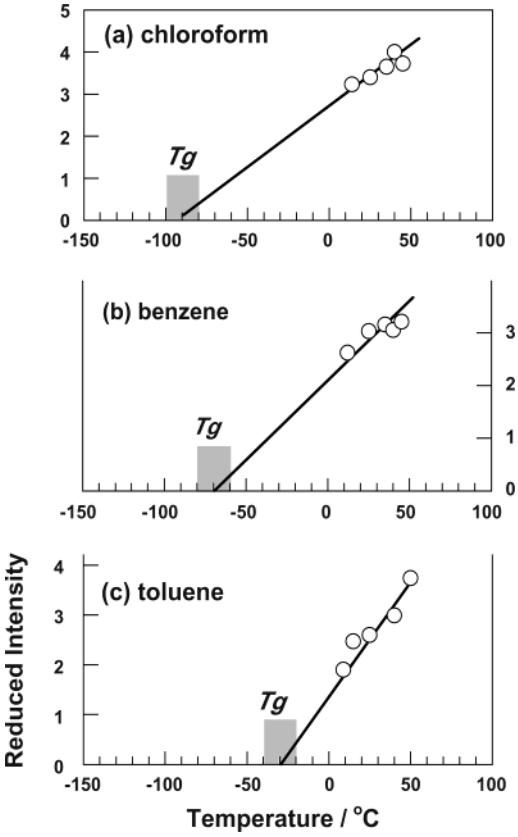

Figure 3. Temperature dependence of the reduced intensity of the 572 cm^{-1} infrared band evaluated at 40 min after the start of the experiment, which was assumed to be almost saturated as discussed in the text. (a) sPS−chloroform, (b) sPS−benzene, and (c) sPS−toluene. The linear extrapolation to the zero intensity was made, where the uncertainty of extrapolation is shown by a shadow.

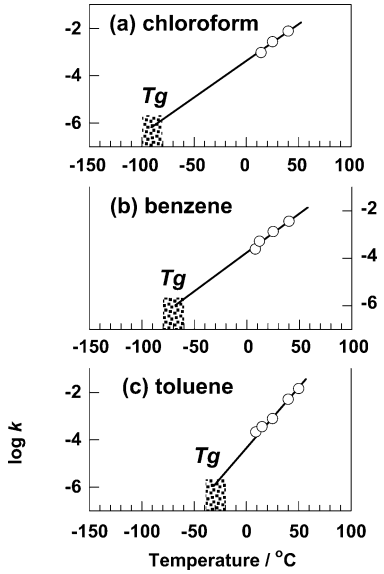

Figure 4. Temperature dependence of the crystallization rate constant k estimated for (a) sPS−chlroform, (b) sPS−benzene, and (c) sPS−toluene systems. The linear extrapolation to the negligibly small k value of 10^{-6} s^{-1} was made to estimate the T_g.

the T_g of −90 ± 10 °C, where the linear correlation coefficient was about 0.99. The result was consistent with the T_g value estimated in Figure 3. (In the previous paper,[42] the extrapolation to the $k = 10^{-5}$ s^{-1} was made for the data of toluene. But this value is still significant,

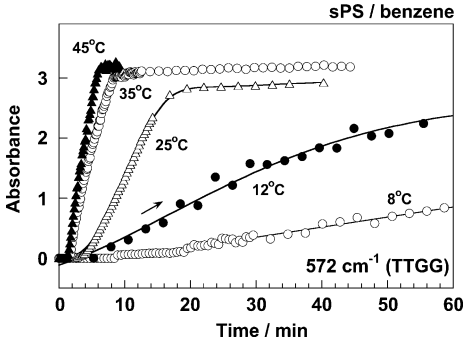

Figure 5. Time dependence of 572 cm^{-1} band intensity plotted at the various temperatures for the sPS−benzene system, where the intensity was reduced by the intensity of the 1150 cm^{-1} standard band.

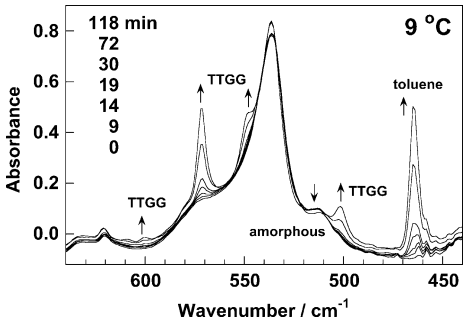

Figure 6. Time dependence of infrared spectra measured in the solvent vapor atmosphere at 9 °C for the sPS−toluene system.

and the 10^{-6} value should be used for getting better correspondence between Figures 3 and 4.) From both Figures 3 and 4, it may be said that the glass transition temperature of sPS was shifted by about 190 °C (from 100 to −90 ± 10 °C) when chloroform is absorbed into the glassy sample.

The similar experiment was made for benzene. Figure 1b shows the time dependence of infrared spectra measured at 40 °C for the sPS−benzene system. Figure 5 shows the time evolution curves of the integrated intensity of 572 cm^{-1} crystalline band evaluated at the various temperatures. The intensity saturated after a long time passage is plotted against the crystallization temperature as shown in Figure 3b. The intensity became lower with decrease in crystallization temperature. The extrapolation to zero crystallinity gave the T_g of −70 ± 10 °C. In parallel, the crystallization rate constant k was estimated from the time dependence of infrared intensity given in Figure 5, and a plot of log k vs temperature was made as shown in Figure 4b. An extrapolation to $k = 10^{-6}$ s^{-1} gives the T_g of ca. −70 ± 10 °C, close to the value obtained in Figure 3.

Similar treatment was made for toluene. The time dependence of infrared spectra measured at 9 °C for the sPS−toluene system is shown in Figure 6. The integrated intensity of the 572 cm^{-1} band was plotted against time as shown in Figure 7. The plot of log k vs temperature, obtained from the Avrami's plot, was already reported in the previous paper.[42] Extrapolation to $k = 10^{-6}$ s^{-1} gives the T_g of −30 ± 10 °C as shown in Figure 4c. A plot of saturated intensity of the 572 cm^{-1} infrared band was made against the crystallization temperature, and an extrapolation to zero crystallinity gives a similar T_g value (Figure 3c).

From these data analyses the solvent-induced T_g shift is found to be largely dependent on the kind of solvent.

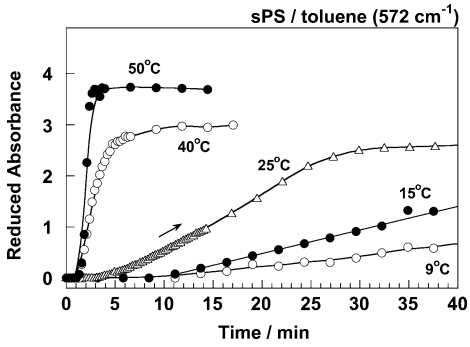

Figure 7. Time dependence of 572 cm^{-1} band intensity plotted at the various temperatures for the sPS−toluene system, where the intensity was reduced by the intensity of the 1150 cm^{-1} standard band.

The largest shift of T_g was observed for chloroform (from 100 to −90 °C), the next largest shift was for benzene (from 100 to −70 °C), and the smallest shift for toluene (from 100 to −30 °C). In the previous papers we compared the crystallization rate measured at room temperature between these three kinds of solvent: chloroform > benzene > toluene.[28,31] The T_g shift has a similar tendency. As for the T_g shift in a mutually miscible two components system, we know various empirical equations. For example, the Fox equation gives the T_g of the miscible blend between the components A and B as $1/T_g = w_A/T_g(A) + w_B/T_g(B)$, where $T_g(i)$ is the T_g of the component i and w_i is the corresponding weight fraction.[43] If we assume that a smaller molecule may have a lower T_g, chloroform should have the lowest T_g, benzene the next higher T_g, and toluene the highest T_g, judging from the effective molecular size (the effective volume is 61 $Å^3$ for chloroform, 73 $Å^3$ for benzene, and 86 $Å^3$ for toluene). Therefore, if the weight fraction of the solvent molecules in the sPS amorphous region is assumed to be the same, the T_g of the sPS−solvent amorphous system should be lower in order of chloroform < benzene < toluene, as actually observed in the present experiment. But, unfortunately, we do not know the weight fractions of the solvent molecules included in the sPS amorphous region and also the T_g's of these solvents. Anyway, it should be noticed that the crystallization rate and the glass transition temperature of sPS amorphous phase are affected very much by the existence of solvent molecules.

Crystallization Induction Time and Critical Sequence Length. In Figures 2, 5, and 7 the integrated intensity of the crystalline band at 572 cm^{-1} was plotted against time. This band started to appear after some induction time since the supply of solvent vapor. But, as reported in the previous papers,[28,30,31,34] this induction time is differently observed when the plot is made for the various infrared bands with different critical sequence length m. The infrared band has its own m value, and the band can be detected for the first time when the regular helix length is beyond this critical value.[44] The 572 cm^{-1} band has a relatively large m value.[31] The infrared band with smaller m value should be observed at earlier stage of crystallization. Since the crystallization rate is lower at a lower temperature, the difference in detection timing of the various bands with different m values may be detected more clearly at lower temperature. Figure 8 shows the semilogarithmic plot of integrated intensity of the two types of bands with different m values: one was the 572 cm^{-1} band with

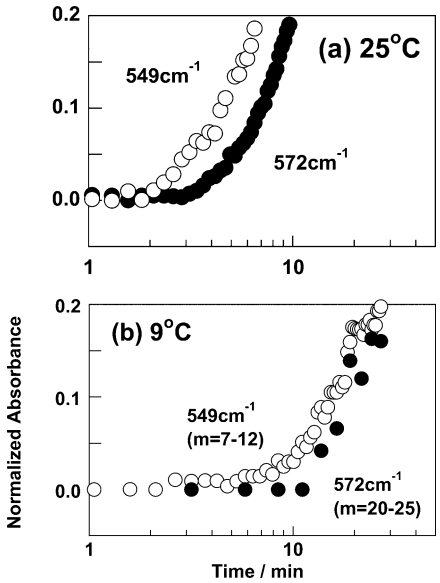

Figure 8. Time dependence of the normalized intensity of the infrared bands with short (549 cm^{-1}) and long critical sequence length (572 cm^{-1}) observed for the sPS−toluene system in the early crystallization stage at (a) 25 and (b) 9 °C.

m = 20−25 monomeric units, and the other was the 549 cm^{-1} band with m = 7−12 monomeric units. At 25 °C the 572 cm^{-1} band appeared around 3 min after the supply of toluene vapor, just when the 549 cm^{-1} band appeared already (about 1 min earlier) and began to grow. At 9 °C the induction time was longer than at 25 °C, and the 549 cm^{-1} band was started to appear at about 6 min and the 572 cm^{-1} band appeared around 11 min after the solvent supply. As discussed in the previous papers,[31−34] the appearance of infrared band with short critical sequence length is considered to correspond to the formation of nuclei consisting of short helical segments. The time gap to detect the bands with different critical sequence lengths tells us that the regular helical segments are growing during this time gap. Figure 8 indicates that both of the nucleation and growth rates of the regular helical segments are slowing down at a lower crystallization temperature.

Figure 9 shows the time dependence of the infrared intensities of the various crystalline bands and the half-width of the 536 cm^{-1} amorphous band estimated at 9 °C. In the previous paper[34] we made a similar plot for the data collected at room temperature. The data at 9 °C showed essentially the same behavior. Immediately after the supply of toluene, the half-width of the amorphous band started to increase (and the peak position shifted to lower frequency side), indicating an occurrence of micro-Brownian motion in the amorphous region. Around 6 min the intensity of the 549 cm^{-1} band with shorter critical sequence length started to increase in intensity, indicating the start of formation of short helical segments as a result of activated motion in the amorphous region. Around 11 min the intensity of the 572 cm^{-1} band with longer critical sequence length increased. Therefore, between 6 and 11 min, the length of regular helical segments increased. Although the X-ray diffraction was not measured at 9 °C, it is considered reasonably that the crystal lattice consisting of these longer helical segments is formed at this timing as described in the previous paper.[34] After that, the half-width of the amorphous band started to decrease and the peak frequency increased. This is because the

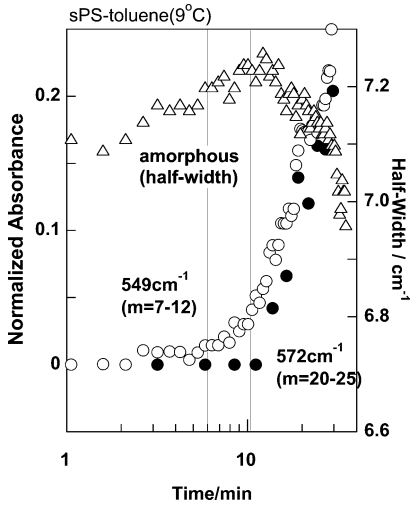

Figure 9. Time dependence of the relative intensity of the various infrared bands and the half-width of the amorphous band (536 cm^{-1}) observed in the early stage of crystallization for the sPS−toluene system at 9 °C.

amorphous chains sandwiched between the crystalline domains become less mobile as the crystalline domains grow furthermore. In this way the structural formation process at 9 °C was extracted concretely from the infrared data, the characteristic feature of which was essentially the same as that observed at room temperature. As discussed already, the time scale of such a structural formation was longer at 9 °C than at room temperature as known from the slowing down of the crystallization rate and the longer induction time.

Molecular Dynamics Simulation of T_g Shift. To check the effect of the sPS−solvent interaction on the T_g shift, the molecular dynamics (MD) simulation was performed for the systems of sPS−toluene and sPS−chloroform. An amorphous chain model was built by using an amorphous builder of Cerius[2] (version 4.6, Accelrys Inc.): one chain consisted of 80 monomeric units including hydrogen atoms. The chain was enclosed in a three-dimensional unit cell, and the ends of the chain were connected between the adjacent cells. Toluene or chloroform molecules were put into the cell at a ratio of styrene units/solvent molecules of 80/0, 80/10, or 80/20. The solvent molecules were input at random into the sPS amorphous cell. The thus-constructed models were energetically minimized at first and then transferred to the MD calculation at the various constant temperatures under the 3-dimensional periodic boundary condition. The potential functions used here were COMPASS.[45] The total time of calculation was 100 ps, and the trajectory was saved at every 50 fs where the time interval of MD calculation was 1 fs.

The time-averaged total volume of the amorphous cell was plotted against temperature as shown in Figure 10 for sPS and sPS−toluene systems. In the case of pure sPS, the two different models gave essentially the same results as indicated by open circle and open triangle symbols. The total volume averaged between them (solid circles) was found to expand almost linearly with increasing temperature. The deflection point was detected around 470 K, which was assumed to correspond to the T_g of sPS random chain. This value was ca. 100 °C higher than the actually observed one, probably coming from the hard potential function parameters used in the calculation. When toluene molecules were supplied to the sPS system at a molar ratio of 80/10,

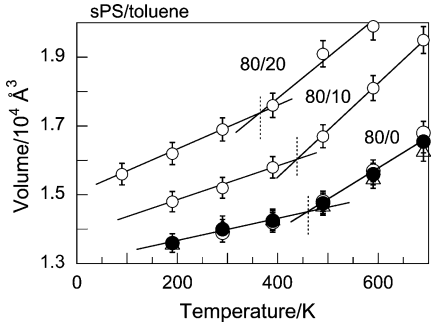

Figure 10. Temperature dependence of the MD unit cell volume calculated for the sPS and sPS−toluene systems. The deflection point corresponds to the T_g. For sPS the two different models were employed in the calculation (open circle and open triangle), but they showed essentially the same result. The values averaged for these two models are shown also by solid circle. The vertical bar indicates the estimated standard error.

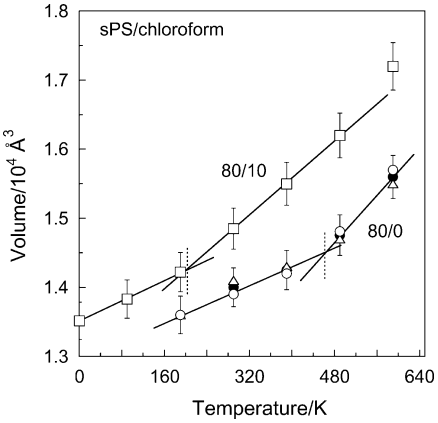

Figure 11. Temperature dependence of the MD unit cell volume calculated for the sPS−chloroform system.

the cell volume increased and the deflection point was detected around 430 K. Further addition of toluene solvent (80/20) shifted the T_g to lower temperature, ca. 370 K. The plasticizing effect can be detected quite clearly. The shift of T_g caused by the supply of toluene was about 100 °C, consistent with the observed shift of ca. 130 °C, although it is unknown which molar ratio of styrene/solvent (80/10 or 80/20) is good for comparison between the observed and calculated results.

Figure 11 shows the case of the sPS−chloroform system. The T_g was detected at about 200 K when chloroform molecules were supplied to sPS system even at a molar ratio of 80/10, a more remarkable T_g shift compared with the case of toluene. The T_g value, −73 °C, obtained by simulation happened to be rather close to the observed data (ca. −90 °C), but the calculated T_g shift of about 270 °C (from 197 to −73 °C) is an overestimation when compared with the actually observed result, 190 °C.

In this way the plasticizing effect of solvent can be reproduced by the MD calculation, and the difference in T_g shift between toluene and chloroform was simulated relatively reasonably though the T_g value of the pure sPS system and its shift were more or less overestimated. More detailed discussion about the atomistic mechanism of the plasticizing effect will be made elsewhere on the basis of the MD calculation result. By performing this type of calculation for much longer time, random coils may be regularized to transform to regular helical sequences. We are now performing this longer MD calculation at the various temperatures.

Conclusions

In the present paper the effect of absorbed organic solvent on the crystallization behavior of sPS system has been investigated by performing the time-resolved infrared spectral measurement at the various temperatures. The infrared data were analyzed on the basis of Avrami's equation, and the glass transition temperature was estimated as a point at which the crystallization did not occur any more and the crystallinity was zero. The solvent-induced T_g shift was found to be the largest for chloroform, the next largest for benzene, and the smallest for toluene among the three kinds of organic solvents investigated in the present study. It is surprising to notice that the T_g was shifted by 130−180 °C due to the solvent effect. The MD calculation gave the relatively good reproduction of these T_g shifts, although the absolute values of T_g and its shift were overestimated possibly due to the hard potential function parameters used in the calculations. The lowering in the T_g means an enhancement of molecular motion of sPS chain in the solvent atmosphere, which should result in the formation of regular helix after long time passage. The next problem that we should solve by the MD calculation is to simulate this conformational regularization by performing the calculation in a much longer time range.

Acknowledgment. The authors thank the Idemitsu Petrochemical Co., Ltd., Japan, for supplying sPS samples.

References and Notes

(1) Reynolds, N. M.; Stidham, H. D.; Hsu, S. L. *Macromolecules* **1991**, *24*, 3662.
(2) Guerra, G.; Vitagliano, V. M.; de Rosa, C.; Petraccone, V.; Corradini, P. *Macromolecules* **1990**, *23*, 1539.
(3) De Rosa, C.; Guerra, G.; Petraccone, V.; Corradini, P. *Polym. J.* **1991**, *23*, 1435.
(4) Sun, Z.; Miller, R. L. *Polymer* **1993**, *34*, 1963.
(5) Corradini, P.; de Rosa, C.; Guerra, G.; Napolitano, R.; Petraccone, V.; Pirozzi, B. *Eur. Polym. J.* **1994**, *30*, 1173.
(6) De Rosa, C. *Macromolecules* **1996**, *29*, 8460.
(7) St. Lawrence, S.; Shinozaki, D. M. *Polym. Eng. Sci.* **1997**, *37*, 1825.
(8) Cartier, L.; Okihara, T.; Lotz, B. *Macromolecules* **1998**, *31*, 3303.
(9) Woo, E. M.; Sun, Y. S.; Lee, M. L. *Polymer* **1999**, *40*, 4425.
(10) Vittoria, V.; Russo, R.; de Candia, F. *Polymer* **1991**, *32*, 3371.
(11) Vittoria, V.; Filho, A. R.; de Candia, F. *Polym. Bull. (Berlin)* **1991**, *26*, 445.
(12) Wang, Y. K.; Savage, J. D.; Yang, D.; Hsu, S. L. *Macromolecules* **1992**, *25*, 3659.
(13) Chatani, Y.; Shimane, Y.; Inagaki, T.; Ijitsu, T.; Yukinari, T.; Shikuma, H. *Polymer* **1993**, *34*, 1620.
(14) Chatani, Y.; Inagaki, T.; Shimane, Y.; Shikuma, H. *Polymer* **1993**, *34*, 4841.
(15) De Candia, F.; Cartenuto, M.; Guadagno, L.; Vittoria, V. *J. Macromol Sci., Phys.* **1996**, *B35*, 265.
(16) De Rosa, C.; Guerra, G.; Petraccone, V.; Pirozzi, B. *Macromolecules* **1997**, *30*, 4147.
(17) Guerra, G.; Manfredi, C.; Musto, P.; Tavone, S. *Macromolecules* **1998**, *31*, 1329.
(18) Moyses, S.; Sonntag, P.; Spells, S. J.; Laveix, O. *Polymer* **1998**, *39*, 3537.
(19) Rastogi, S.; Goossens, J. G. P.; Lemstra, P. J. *Macromolecules* **1998**, *31*, 2983.
(20) Guadagno, L.; Baldi, P.; Vittoria, V.; Guerra, G. *Macromol. Chem. Phys.* **1998**, *199*, 2671.
(21) Tsutsui, K.; Tsujita, Y.; Yoshimizu, H.; Kinoshita, T. *Polymer* **1998**, *39*, 5177.
(22) Goossens, H.; Rastogi, S.; Lemstra, P. *Macromol. Symp.* **1999**, *138*, 99.
(23) De Rosa, C.; Rizzo, P.; de Ballesteros, O. R.; Petraccone, V.; Guerra, G. *Polymer* **1999**, *40*, 2103.
(24) Tsutsui, K.; Katsumata, T.; Fukatsu, H.; Yoshimizu, H.; Kinoshita, T.; Tsujita, Y. *Polym. J.* **1999**, *31*, 268.
(25) Tsutsui, K.; Katsumata, T.; Yamamoto, Y.; Fukatsu, H.; Yoshimizu, H.; Kinoshita, T.; Tsujita, Y. *Polymer* **1999**, *40*, 3815.
(26) Moyses, S.; Spells, S. J. *Macromolecules* **1999**, *32*, 2684.
(27) Moyses, S.; Spells, S. J. *Polymer* **1999**, *40*, 3269.
(28) Tashiro, K.; Ueno, Y.; Yoshioka, A.; Kaneko, F.; Kobayashi, M. *Macromol. Symp.* **1999**, *141*, 33.
(29) Musto, P.; Manzari, M.; Guerra, G. *Macromolecules* **2000**, *33*, 143.
(30) Tashiro, K.; Sasaki, S.; Ueno, Y.; Yoshioka, A.; Kobayashi, M. *Korea Polym. J.* **2000**, *8*, 103.
(31) Tashiro, K.; Ueno, Y.; Yoshioka, A.; Kobayashi, M. *Macromolecules* **2001**, *34*, 310.
(32) Daniel, C.; Guerra, G.; Musto, P. *Macromolecules* **2002**, *35*, 2243.
(33) van Hooy-Corstjens, C. S. J.; Magusin, P. C. M. M.; Rastogi, S.; Lemstra, P. J. *Macromolecules* **2002**, *35*, 6630.
(34) Tashiro, K.; Yoshioka, A. *Macromolecules* **2002**, *35*, 410.
(35) Gowd, E. B.; Nair, S. S.; Ramesh, C. *Macromolecules* **2002**, *35*, 8509.
(36) Milano, G.; Guerra, G.; Muller-Plathe, F. *Chem. Mater.* **2002**, *14*, 2977.
(37) Mori, S.; Amutharani, D.; Yamamoto, Y.; Tsujita, Y.; Yoshimizu, H. *Polym. Prepr. Jpn.* **2002**, *51*, 2592.
(38) Tashiro, K.; Yoshioka, A. *Macromolecules* **2003**, *36*, 3001.
(39) Yoshioka, A.; Tashiro, K. *Macromolecules* **2003**, *36*, 3593.
(40) Gowd, E. B.; Nair, S. S.; Ramesh, C. *Macromolecules* **2002**, *35*, 8509.
(41) Gowd, E. B.; Nair, S. S.; Ramesh, C.; Tashiro, K. *Macromolecules* **2003**, *36*, 7388.
(42) Yoshioka, A.; Tashiro, K. *Polymer* **2003**, *44*, 6681.
(43) Fox, T. *Bull. Am. Phys. Soc.* **1956**, *1*, 123.
(44) Kobayashi, M.; Akita, K.; Tadokoro, H. *Makromol. Chem.* **1968**, *118*, 324.
(45) Sun, H. *J. Phys. Chem. B* **1998**, *102*, 7338.

MA035505Z